Viewpoint Paper

Microstructural refinement and property enhancement of cast light alloys via friction stir processing

Z.Y. Ma,[a,*] A.L. Pilchak,[b] M.C. Juhas[b,1] and J.C. Williams[b]

[a]*Institute of Metal Research, Chinese Academy of Sciences, 72 Wenhua Road, Shenyang 110016, China*
[b]*Department of Materials Science and Engineering, The Ohio State University, Columbus, OH 43210, USA*

Abstract—Friction stir processing (FSP) is a novel metal-working technique that provides microstructural modification and control in the near-surface layer of metal components. FSP of cast Al and Mg alloys resulted in the break-up of coarse dendrites and secondary phases, refinement of matrix grains, dissolution of precipitates and elimination of porosity, thereby improving the mechanical properties of the castings significantly. Cast Ti alloys do not contain harmful secondary phases and the dendritic structure is masked by the β to α allotropic transformation, but the coarse lamellar structure is undesirable. In this article, microstructure and particle refinement, accelerated dissolution of precipitates and alloy systems suitable for FSP were addressed.
© 2007 Acta Materialia Inc. Published by Elsevier Ltd. All rights reserved.

1. Introduction

The idea of locally tailoring microstructure to optimize a particular property is not new. The challenge has been to identify practical ways of implementing this idea. Starting with the work on aluminum alloys by Mishra et al. [1] and continuing with navy bronzes by Mahoney et al. [2], the use of friction stir processing (FSP) appears to hold the promise of realizing this goal of locally altering the microstructure. The use of FSP to locally refine the intrinsically coarse microstructure of castings has particular appeal. This is particularly attractive in situations where strength or fatigue crack initiation is the limiting property of castings.

Consequently, it seems realistic to suggest that FSP can be used to selectively enhance the fatigue crack initiation resistance in locations of high cyclic stress. It would be economically unrealistic to treat the entire surface by FSP, but the likelihood of this being necessary seems low anyway. Clearly, further work to achieve reduction in practice is required, but the use of FSP for this purpose appears to have no intrinsic technical barriers, making it a viable option for design engineers

concerned about fatigue limitations. This article focuses on FSP-induced microstructural modification of cast light alloys, i.e., cast aluminum and magnesium alloys, and a cast + hot isostatic pressed (HIP) titanium alloy. Particular attention was paid to the level of grain and particle refinement, the accelerated dissolution of precipitates and the alloy systems suitable for FSP.

2. Cast aluminum alloys

Al–Si–Mg (Cu) alloys are widely used to cast high-strength components in the aerospace and automobile industries. However, porosity, coarse acicular Si particles and coarse primary aluminum dendrites in the cast structure (Fig. 1a) reduce the mechanical properties of the castings, in particular the ductility, toughness and fatigue strength [3,4]. Eutectic modifiers and high-temperature heat treatment, widely used to modify the cast microstructure [5–7], cannot eliminate the porosity effectively and redistribute the Si particles uniformly. FSP has been proven to be a very effective route to enhance the mechanical properties of cast Al–Si alloys. The functions of FSP are: (i) to break-up the coarse Si particles and disperse them into the matrix; (ii) to break-up the coarse aluminum dendrites and refine the grain structure; (iii) to break-up the coarse precipitates and dissolve

---

* Corresponding author. Tel./fax: +86 24 83978908; e-mail: zyma@imr.ac.cn
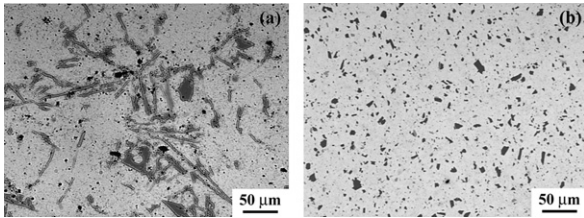[1] Currently on leave at The National Science Foundation.

Figure 1. Optical microstructure of A356 samples: (a) as-cast, (b) two-pass FSP, 900 rpm–203 mm min^{-1}.

part or most of them into the matrix; and (iv) to eliminate the casting porosity.

2.1. Main influential factors

At lower tool rotation rates or rotation rate/traverse speed ratios, i.e., under lower heat input conditions, a macroscopically visible banded structure with a low density of large Si particles was observed in FSP A356 samples [8]. The increase in the rotation rate or the rotation rate/traverse speed ratio led to the elimination of the banded structure [8]. Further, this resulted in a reduced Si particle size and porosity level, and an increased amount of dissolved Mg_2Si phase [9]. This is because FSP with a higher heat input intensifies frictional heating and stirring, consequently creating a higher temperature in the stir zone (SZ) and subsequently more thorough material mixing and a more uniform distribution of Si particles. Two-pass FSP with a 100% overlap produced a better effect (Fig. 1b) [9].

Significant microstructural refinement, homogeneity and densification by FSP in A356 castings resulted in remarkable improvement in the tensile properties and fatigue strength [9,10]. Increasing the rotation rate or FSP pass resulted in enhanced mechanical properties, due to the reduced Si particle size and porosity level, and increased dissolution of Mg_2Si [9]. Post-FSP aging increased the strength of the FSP A356 samples further (Table 1). This indicates that part or most of the Mg_2Si phase was dissolved into the aluminum matrix during FSP and most of the solutes remained in solution due to rapid cooling from FSP temperature. The accelerated dissolution of the precipitates during FSP is discussed in Section 3.2. Two-pass FSP + aging produced a tensile strength of 304 MPa and a yield strength of 236 MPa

with excellent ductility in the cast A356 sample. This indicates that a combination of optimized FSP parameters and post-FSP aging can produce maximum strengthening in the cast A356 sample.

2.2. Achievable refining level of Si particles and grains

For sand-cast A356 alloys, FSP resulted in the generation of a uniform fine-grained structure of 5–8 μm, with the uniformly distributed fine Si particles having an average size of 2–3 μm and an average aspect ratio of ∼2.0 [9]. At higher tool rotation rates, the size and aspect ratio of the Si particles tended to decrease due to the more intense stirring effect. However, a rotation rate above 1000 rpm did not result in any further refinement of the Si particles [9]. This may be associated with of obviously improved matrix flowability under higher heat input conditions, where the break-up of the Si particles would not be further intensified because it became easy for the particles to flow with the flow deformation of the matrix. Two-pass or multiple-pass FSP with a 100% overlap is a feasible approach to achieve a further refinement of the Si particles [9].

For chemically modified A356 samples, FSP resulted in break-up and dispersion of fibrous Si particles, creating a uniform microstructure with a grain size of 3–4 μm and an Si particle size of 0.2–0.5 μm [8]. Increasing the rotation rate did not increase the size of the recrystallized grains obviously due to the effective pinning effect of the fine Si particles [8]. Therefore, a relatively fine grain structure could be obtained. Similarly, Nakata et al. [11] produced a fine grain structure of 2–3 μm in ADC12 die casting alloy via FSP.

2.3. Alloy systems suitable for FSP

The mechanical properties of the A356 castings can be significantly enhanced via FSP due to the break-up and dispersion of the coarse Si particles, matrix grain refinement and porosity closure, and they are further improved by post-FSP aging strengthening resulting from the dissolved Mg_2Si phase. Therefore, Al–Si–Mg(Cu) cast alloys containing coarse Si particles and precipitates are very suitable alloy systems for FSP.

For high-strength 7xxx and 2xxx series alloys, a fine-grained structure can be obtained from the castings via FSP. It is proper to use FSP to produce the fine-grained superplastic aluminum alloys.

3. Cast magnesium alloys

Mg–Al–Zn alloys with a higher Al content are widely used as die-cast or wrought alloys, e.g., AZ91 and AZ80. The as-cast structure is characterized by coarse α-Mg dendrites and a network-like eutectic β-$Mg_{17}Al_{12}$ phase along the grain boundaries (Fig. 2a). Conventionally, a solution treatment (ST) at ∼415 °C for up to 40 h followed by an aging is used to modify the morphology and distribution of the β-phase to enhance the mechanical properties. However, such a procedure is time consuming, resulting in not only increased material cost but also surface oxidation and grain coarsening.
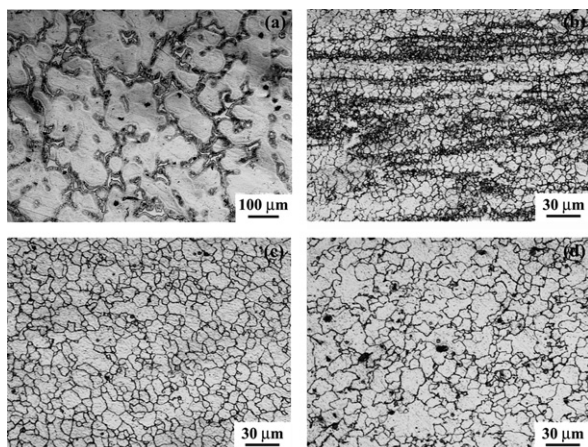
Table 1. Tensile properties of cast and FSP A356 (900 rpm–203 mm/min) and AZ91 (400 rpm–100 mm/min) samples under various conditions

Materials	Conditions	YS (MPa)	UTS (MPa)	El. (%)
A356[a]	As-cast/T6 PM	132/210	169/220	3/2
	As-FSP/aged	140/202	232/275	38/30
	Two-pass FSP/aged	162/236	255/304	34/25
AZ91	As-cast/T6 PM	75/92	101/185	2.5/8.2
	As-FSP/aged	140/–	248/–	8.7/–
	Pre-ST + FSP/aged	–/154	–/285	–/6.8
	Two-pass FSP/aged	125/177	327/337	20/10

[a] Tensile properties were obtained by using mini-tensile specimens.

Figure 2. Optical microstructure of AZ91 magnesium alloy: (a) as-cast, (b) single-pass FSP, (c) single-pass FSP with a pre-ST and (d) two-pass FSP (400 rpm–100 mm min^{-1} for all FSP samples).

FSP has two main functions. The first is to refine, homogenize and densify the microstructure. The second is to dissolve the β-phase into the magnesium matrix. Because of the very low diffusion rate of the solutes in magnesium, air cooling can prevent the precipitation of the solutes in a supersaturated magnesium solid solution. Thus, FSP has the function of the ST.

3.1. Main influential factors

When an as-cast structure was used for FSP, onion rings, associated with β-particle bands and non-uniform grain regions, were distinctly visible in the SZ of the FSP AZ91 sample at 400 rpm (Fig. 2b). This is attributed to the lower strain rate/strain and temperature conditions. By increasing the rotation rate from 400 to 600 rpm, the onion rings tended to disappear [12]. Clearly, at a very high rotation rate, a uniform microstructure and the fundamental dissolution of the β-phase are likely to be achieved. However, the higher heat input will result in remarkable grain coarsening. This will cause deterioration of the mechanical properties of the FSP samples.

One of the solutions is to change the starting structure to enhance the flowability of the material. Cavaliere and De Marco have used a 415 °C/2 h pre-ST to soften AZ91 prior to FSP [13]. A recent study [12] showed that the flow characteristics of as-cast AZ91 were obviously improved by a 415 °C/16 h pre-ST which dissolved most of the β-phase. In this case, FSP with a lower rotation rate of 400 rpm could create a fine and uniform microstructure (Fig. 2c). However, the pre-ST made the FSP modification procedure complex and costly, and obviously reduced its practical value.

Alternatively, multiple-pass FSP with a 100% overlap is an effective approach to achieve the microstructural refinement and homogeneity. A two-pass FSP at 400 rpm produced a fine and uniform microstructure in as-cast AZ91 (Fig. 2d), with 89% of the β-phase being dissolved [14], indicating that two-pass FSP produced a solid solution effect.

FSP resulted in significantly enhanced mechanical properties (Table 1). With a two-pass FSP, the tensile strength and ductility were further enhanced due to in-creased β-phase dissolution and improved microstructural homogeneity (Fig. 2). Post-FSP aging resulted in a significant increase in strength and a reduction in ductility due to the precipitation of fine β-particles [14]. Under the post-FSP aging condition, the mechanical properties of the two-pass FSP AZ91 sample exceeded those of the single-pass FSP sample with a 415 °C/16 h pre-ST. Therefore, two-pass FSP + aging can be established as an effective approach to enhance the mechanical properties of cast Mg–Al–Zn alloys.

3.2. Accelerated dissolution phenomenon

For Mg–Al alloys, the interdiffusion coefficient $\widetilde{D}$ can be expressed by [15]

$$\widetilde{D} = 3.39 \times 10^{-4} \ \text{m}^2 \ \text{s}^{-1} \cdot \exp\left(\frac{-135 \ \text{kJ/mol}}{RT}\right) \qquad (1)$$

where R is the gas constant and T is the absolute temperature. The time needed for a diffusion distance d can be estimated by the relationship $t = d^2 \widetilde{D}^{-1}$ [15]. For as-cast AZ91 and AZ80 alloys, the typical grain size is ~100–200 μm (Fig. 2a). Supposing that the diffusion distance for aluminum is 50 μm, it will take ~37 h to complete the diffusion at 415 °C.

During FSP, the rotating threaded pin induces severe plastic deformation in the SZ with a strain rate of 10^0–10^2 s^{-1} and a strain of up to ~40 [16,17], resulting in intense break-up and mixing of α-Mg and β-phase. In this case, the diffusion distance for aluminum is significantly shortened. If we assume that the diffusion distance of aluminum is 0.5 μm during FSP, then it takes only ~13 s to complete the diffusion at 415 °C. On the other hand, the high dislocation density is introduced by severe plastic deformation during FSP [18], and this allows the occurrence of pipe diffusion. Based on the calculations using the data in Ref. [19], the pipe diffusion rate is at least 1000 times higher than the bulk one for magnesium. Thus, for the same diffusion distance, the time needed for complete dissolution is shortened by at least 1000 times. Chang et al. [16] recorded maximum temperature of 300–420 °C during FSP of AZ31 by embedding thermocouples ~2.5 mm below the rotating pin. The actual temperature in the SZ is higher than that recorded by the thermocouples. Therefore, it is very likely to achieve the dissolution of most of the β-phase during FSP due to the significantly accelerated diffusion rate and shortened diffusion distance.

3.3. Achievable grain refining level

In the AZ and AM alloys containing the β-phase, FSP produced a supersaturated solid solution with hardly any second-phase particles due to the dissolution of most of the β-phase. In this case, the coarsening of the recrystallized grains was inevitable during FSP due to the absence of pinning particles. Therefore, the grain size obtained in the FSP magnesium alloys was usually on the order of 8–20 μm and larger than that in the FSP aluminum alloys.

According to the dynamic recrystallization theory, it is possible to obtain finer grains in the FSP AZ and AM

alloys by decreasing the heat input. However, this will generate a non-uniform microstructure and reduce the amount of dissolved β-phase. Based on previous studies [12,14], a two-pass or multiple-pass FSP with varied parameter combinations is suggested. The first FSP pass is conducted under a higher heat input to break and dissolve the β-phase and homogenize the microstructure. The subsequent FSP pass is performed under a lower heat input to refine the grain structure.

For heat-resistant magnesium alloys, it is possible to obtain a very fine grain structure by FSP. For example, FSP of 2 mm thick Mg–6Al–3Ca thixomolded plate at 1500 rpm and 1500 mm min^{-1} resulted in the break-up and dispersion of Al$_2$Ca networks, producing a fine grain structure of 0.8–1.0 μm with uniformly distributed fine Al$_2$Ca particles of 20–100 nm [20]. This was mainly attributed to the existence of the fine and stable Al$_2$Ca pinning particles and the higher traverse speed, corresponding to the higher strain rate and lower thermal input.

3.4. Alloy systems suitable for FSP

FSP in Mg alloys can achieve a dual purpose, i.e., refine/homogenize the as-cast structure and dissolve the β-phase. A combination of optimized FSP parameters and post-FSP aging enhances the mechanical properties significantly. Therefore, Mg alloys containing the coarse β-phase are very suitable alloy systems for FSP.

For Mg–Zn–Zr (ZK) alloys, the as-cast structure is characterized by pseudo-eutectoid (Mg$_3$Zn$_2$ + α-Mg) distributed along the grain boundaries. It is likely to refine/homogenize the as-cast structure and dissolve the Mg$_3$Zn$_2$ phase in the ZK alloys via FSP. It was reported that FSW of extruded ZK60 plate resulted in the dissolution of most of the MnZn phase and the generation of a fine grain structure of ∼5 μm [21].

For as-cast heat-resistant magnesium alloys, thermally stable particles such as Al$_2$Ca, Mg$_3$Zn$_6$Y, Mg$_3$Zn$_3$Y$_2$ and Mg$_{14}$Nd$_2$Y are coarse and non-uniformly distributed. A high-temperature heat treatment that modifies the morphology and distribution of the particles is not recommended due to significant grain coarsening. By using FSP, these particles are broken up and dispersed with significantly refined grains [20,22].

4. Cast Ti–6Al–4V

There has been growing acceptance of near-net shape structural castings, most often Ti-6-4, in the aerospace industry. However, the coarse as-cast or as-cast and HIP microstructure does not have fatigue crack initiation resistance equivalent to that of wrought products [23]. FSP can be used to refine the cast microstructure to increase fatigue crack initiation resistance.

4.1. Refinement of the as-cast lamellar structure

The coarse colony microstructure (∼1 mm prior β grains and 500 μm colonies) is completely eliminated during α/β- and β-FSP and replaced by either 1 μm equiaxed α grains or ∼15 μm α colonies in 30 μm prior β

grains, respectively, [24]. The designations α/β- and β- refer to the constitution of the SZ at the peak temperature during processing. The SZ temperature is controlled the same way as in Al alloys, by adjusting tool rotation/ tool traverse ratios. The lower thermal conductivity of Ti also makes plunge depth a more important factor. Mechanisms based on continuous recrystallization (CR) have been proposed for grain refinement in aluminum alloys. A similar mechanism is likely operative during FSP cast Ti-6-4. CR processes rely on progressive recovery processes to form low angle boundaries that gradually increase their misorientation as dislocation density increases or by sub-grain coalescence. The former is more likely during high strain and strain rate processing.

There is temperature that gradient extends several millimeters ahead of the tool [25,26], while the instantaneous strain gradient across the transition zone (TZ) only ranges from a few to several hundred microns [27]. As the tool traverses the as-cast structure the volume fraction of β ahead of the tool increases and the α lamellae become narrower. This is important since the recrystallized grain size is generally limited by the α lamellae width at the deformation temperature [28].

The TZ contains the most valuable information with regards to the initial deformation behavior of the as-cast structure during FSP. It is typically characterized by both deformed colony structure and recrystallized equiaxed α grains in α/β- and β-FSP, although during β-FSP there is a higher volume fraction of transformed β [24] because of the higher peak processing temperature. EBSD maps of the TZ/SZ interface are shown in Figures 3 and 4. A significant fraction of the boundaries in the TZ have low misorientation, while in the adjacent SZ the distribution becomes more uniform. Networks of low angle boundaries (<10°) form sub-grains to accommodate the kinks in the lamellae. The transition from low to high angle boundaries is consistent with continuous recrystallization reactions.

It is also common to retain grains from the base material that are in "stable orientations" after CR processes [29]. The effect is exacerbated in titanium alloys
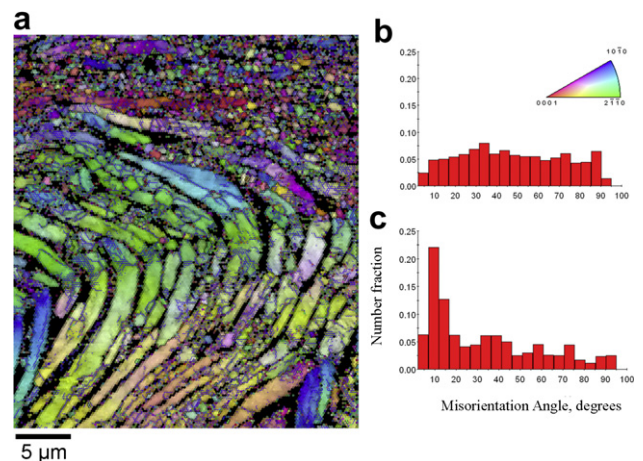

Figure 3. (a) Combined image quality and IPF map acquired with a step size of 0.40 μm. Histograms of the α-phase grain boundary misorientation distributions are shown for the SZ (b) and TZ (c).
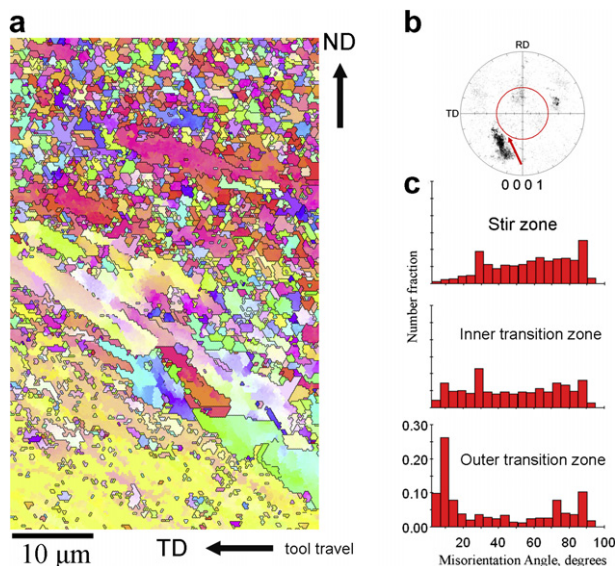
Figure 4. (a) IPF colored EBSD map from a longitudinal section of the TZ. RD points into the page. (b) A discrete 0 0 0 1 pole figure with the maximum shear plane due to the compressive down force superimposed. (c) Misorientation distributions for the SZ and two areas in the TZ.

due to the lower symmetry and plastic anisotropy of the α-phase. Stable orientations in hcp metals are those in which the c-axis is aligned the principal loading direction [30]. This enforces $\langle c + a \rangle$ slip, which has a higher critical resolved shear stress than any of the $\langle a \rangle$ slip systems [31]. The stress state imposed by the friction stir tool is complex, so it is unlikely that the Schmid factor will ever be 0 for all $\langle a \rangle$ slip systems. In Figure 4b, we see that the basal planes in the TZ suitably oriented for slip rotate to an orientation with higher resolved shear stress and these grains recrystallize easily. In Figure 4a, however, there are patches of unrecrystallized grains in stable orientations where [0 0 0 1] is aligned with the maximum shear stress imposed by the rotation of the tool (∥RD). The average grain size in the SZ in Figure 4a is 1.3 μm, which corresponds well with the sub-grain size in the TZ. As comparison, the TZ in cubic materials is often characterized by simple shear [32,33].

As deformation intensifies and material is swept around the FS tool, the applied strain rate must be higher than in the TZ. There is uncertainty about the exact strains and strain rates during FSP of Ti-6-4; however, it is accepted that both values are high compared with those typically encountered in conventional metal-working processes. An interesting feature of the α/β-FSP microstructure is the apparent lack of a deformation texture, which is contradictory to what is commonly observed in CR reactions. This suggests that additional factors must be considered under the high strain and strain rate conditions. These factors are currently not understood, but the essential absence of microtexture in the equiaxed α grains in the SZ is both unexpected and potentially significant. This observation merits further study.

The CR mechanism accounts for formation of equiaxed α grains in the TZ in β-FSP Ti-6-4, but fails to describe the formation of the β grains in the SZ. The peak

processing temperature in the SZ is above the β transus. Consequently, no second-phase is present to pin the β grain boundaries and recrystallization proceeds unimpeded. The substantially refined grain size with a transformed colony structure and the absence of a second-phase to pin β grain boundaries during processing is consistent with dynamic recrystallization. This also supports suggestions regarding FSW of Ti-6-4 [34]. The β grain size is larger than the equiaxed α grain size in the α/β-FSP material because of solute partitioning in the α and β phases and increased diffusion distances limit grain coarsening, while β grain growth kinetics rely on short-range diffusion.

4.2. Mechanical properties of FSP Ti-6-4

It is well established that slip length has a predominant effect on the mechanical properties of Ti-6-4 [35]. Slip length is governed by α colony size in the as-cast (~500 μm) and β-FSP (~15 μm) microstructures, whereas is it controlled by the primary α grain size (~1 μm) in the α/β-FSP material. As a comparison, the primary α grain size in commercially available equiaxed Ti-6-4 is about 10 μm. Yield strength, crack initiation resistance (HCF strength) ductility and the threshold stress intensity range (ΔK_{th}) for microcracks increase as slip length decreases. On the other hand, ΔK_{th} for macrocracks (at $R = 0.1$ and 0.7), FCG resistance and fracture toughness all decrease as slip length decreases [35].

Increases in Ti-6-4 yield strength, crack initiation resistance and fatigue life after FSP have been recently reported [36,37]. The yield stress was evaluated using micropillars created with a focused ion beam while four-point bend fatigue testing assessed the crack initiation resistance and fatigue life at a constant stress amplitude. The FSP samples in the α/β- and β-FSP conditions had fatigue lives over an order of magnitude longer than the as-cast sample [37].

The FS cycle eliminates grain boundary α from the as-cast microstructure, which enhances tensile ductility and stress corrosion resistance. This is especially true in higher strength conditions. The benefits of eliminating grain boundary α would be more pronounced if FSP were applied to higher strength alloys.

5. Summary and outlook

In cast Al and Mg alloys, FSP with higher heat input or multiple-pass resulted in the break-up of coarse dendrites and second-phase particles, refinement of matrix grains, elimination of porosity and dissolution of most of precipitates, thereby creating a fine, uniform and pore-free wrought structure. The accelerated dissolution of the precipitates was attributed to the significantly accelerated diffusion rate and shortened diffusion distance. Post-FSP aging resulted in the precipitation of the dissolved solutes to form fine and uniformly distributed precipitates. Thus, a multiple-pass FSP plus post-FSP aging resulted in a significant enhancement in the mechanical properties of the castings. Heat-treatable Al and Mg cast alloys containing coarse second-phase

particles and precipitates are ideal alloy systems for FSP because FSP produced the dual functions of microstructural modification and solution treatment.

In cast Ti–6Al–4V, FSP led to a significant refinement of the coarse, fully lamellar microstructure. This microstructural refinement led to an increased yield strength and improvement in fatigue crack initiation resistance. The mechanism of microstructural refinement appears to be a variant of continuous recrystallization.

The future efforts on FSP modification of cast light alloys will focus on developing high fidelity robust process models that relate the external process variables (rotation rate, traverse speed, tool geometry, etc.) to the internal response variables (temperature profile, strain rate and strain), and subsequently to the microstructural evolution to be able to predict and tailor the resultant properties in specific casting locations based on FSP input processing parameters.

Acknowledgement

References

[1] R.S. Mishra, M.W. Mahoney, S.X. McFadden, N.A. Mara, A.K. Mukherjee, Scripta Mater. 42 (2000) 163.
[2] M.W. Mahoney, W.H. Bingel, S.R. Sharma, R.S. Mishra, Mater. Sci. Forum. 426 (4) (2003) 2843–2848, Thermec'2003, Pts. 1–5.
[3] D.L. Zhang, L. Zheng, Metall. Mater. Trans. 27A (1996) 3983.
[4] Y.B. Yu, P.Y. Song, S.S. Kim, J.H. Lee, Scripta Mater. 41 (1999) 767.
[5] G. Atxaga, A. Pelayo, A.M. Irisarri, Mater. Sci. Technol. 17 (2001) 446.
[6] K.T. Kashyap, S. Murrall, K.S. Raman, K.S.S. Murthy, Mater. Sci. Technol. 9 (1993) 189.
[7] L. Wang, S. Shivkumar, Z. Metallkd. 86 (1995) 441.
[8] Z.Y. Ma, S.R. Sharma, R.S. Mishra, Mater. Sci. Eng. A433 (2006) 269.
[9] Z.Y. Ma, S.R. Sharma, R.S. Mishra, Metall. Mater. Trans. 37A (2006) 3323.
[10] S.R. Sharma, Z.Y. Ma, R.S. Mishra, M.W. Mahoney, Scripta Mater. 51 (2004) 237.
[11] K. Nakata, Y.G. Kim, H. Fujii, T. Tsumura, T. Komazaki, Mater. Sci. Eng. A437 (2006) 274.
[12] A.H. Feng, Z.Y. Ma, unpublished results.
[13] P. Cavaliere, P.P. De Marco, J. Mater. Process. Technol. 184 (2007) 77.
[14] A.H. Feng, Z.Y. Ma, Scripta Mater. 56 (2007) 397.
[15] S. Kleiner, O. Beffort, P.J. Uggowitzer, Scripta Mater. 51 (2004) 405.
[16] C.I. Chang, C.J. Lee, J.C. Huang, Scripta Mater. 51 (2004) 509.
[17] P. Heurtier, C. Desrayaud, F. Montheillet, Mater. Sci. Forum. 396–402 (2002) 1537.
[18] J.-Q. Su, T.W. Nelson, R. Mishra, M. Mahoney, Acta Mater. 51 (2003) 713.
[19] H.J. Frost, M.F. Ashby, Deformation-mechanism Map, Pergamon Press, Oxford, 1982.
[20] D. Zhang, M. Suzuki, K. Maruyama, Scripta Mater. 52 (2005) 899.
[21] G.M. Xie, Z.Y. Ma, L. Geng, Mater. Sci. Eng. A., in press.
[22] G.M. Xie, Z.Y. Ma, L. Geng, R.S. Chen, Mater. Sci. Eng. A 471 (2007) 63.
[23] D. Eylon, R. Boyer, in: Proceedings of the International Conference on Titanium and Aluminum, Paris, 1990.
[24] A.L. Pilchak, Z.T. Li, J.J. Fisher, A.P. Reynolds, M.C. Juhas, J.C. Williams, in: R.S. Mishra, M.W. Mahoney, T.J. Lienert, K.V. Jata (Eds.), Friction Stir Welding and Processing IV, TMS, Warrendale, PA, 2007, p. 419.
[25] R.L. Goetz, K.V. Jata, in: K.V. Jata, M.W. Mahoney, R.S. Mishra, S.L. Semiatin, D.P. Filed (Eds.), Friction Stir Welding and Processing, Warrendale, PA, USA, TMS, 2001, pp. 35–42.
[26] T.J. Lienert, K.V. Jata, R. Wheeler, V. SeetharamanProceedings of the Joining of Advanced and Specialty Materials, vol. III, ASM International, Materials Park OH, 2001, pp. 160–167.
[27] A.L. Pilchak, M.C. Juhas, J.C. Williams, Metall. Mater. Trans. 38A (2007) 401.
[28] M. Peters, G. Lütjering, G. Ziegler, Z. Metallkd. 74 (1983) 274.
[29] R.D. Doherty, D.A. Hughes, F.J. Humphreys, J.J. Jonas, D.J. Jensen, M.E. Kassner, W.E. King, T.R. McNelley, H.J. McQueen, A.D. Rollett, Mater. Sci. Eng. A 328 (1997) 219.
[30] T.R. Bieler, S.L. Semiatin, Int. J. Plasticity 18 (2002) 1165.
[31] J.C. Williams, R.G. Baggerly, N.E. Paton, Metall. Trans. 33A (2002) 837.
[32] R.W. Fonda, J.F. Bingert, Metall. Trans. 35A (2004) 1487.
[33] K. Oh-Ishi, A.P. Zhilyaev, T.R. McNelley, Metall. Mater. Trans. 37A (2006) 2239.
[34] A.J. Ramirez, M.C. Juhas, Mater. Sci. Forum. 426–432 (2003) 2999.
[35] G. Lütjering, J.C. Williams, Titanium, Springer, New York, 2003.
[36] A.L. Pilchak, D.M. Norfleet, M.C. Juhas, J.C. Williams, in: Materials Behvaior: Far from Equilibrium, Metall. Mater. Trans. A, in press.
[37] A.L. Pilchak, M.C. Juhas, J.C. Williams, in: Proceedings of the 11th World Conference on Titanium, Kyoto, Japan, 2007, in press.